

**COMPARISON OF ELECTRICAL RESISTIVITY OF
SEVERAL CANDIDATE CTR MATERIALS**

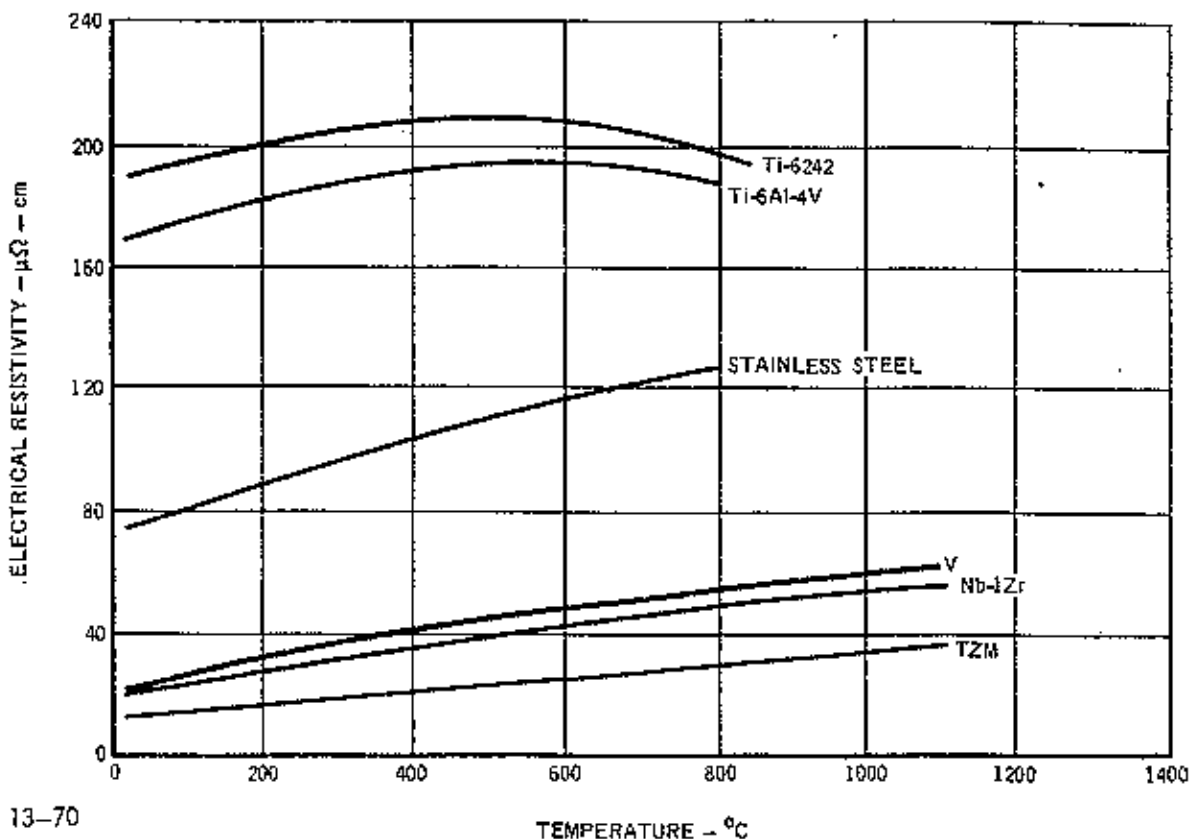


Figure 2

**ESTIMATED VAPOR PRESSURES OF CANDIDATE
FIRST WALL MATERIALS**

CANDIDATE FIRST WALL MATERIAL	PROPOSED MAXIMUM OPERATING TEMPERATURE ($^{\circ}\text{C}$)	ESTIMATED VAPOR PRESSURE (atm)*
ALUMINUM	300	1.34×10^{-47}
TITANIUM	500	2.09×10^{-40}
316 SS	600	1.05×10^{-27}
VANADIUM	800	1.33×10^{-25}
NOBIUM	1000	7.71×10^{-30}
MOLYBDENUM	1000	9.68×10^{-27}

*Based on the data of Reference 7; extrapolated using linear regression analysis of vapor pressure vs reciprocal temperature data.

Table 3

Thermal Stress

$$\sigma_{th} = \frac{\alpha E}{2k(1-\nu)} \left[w_s t + 0.5 w_n t^2 \right]$$

**Material
Related** **Reactor
Related**

α = **coefficient of thermal expansion**

E = **Modulus of Elasticity**

k = **thermal conductivity**

ν = **Poison Ratio**

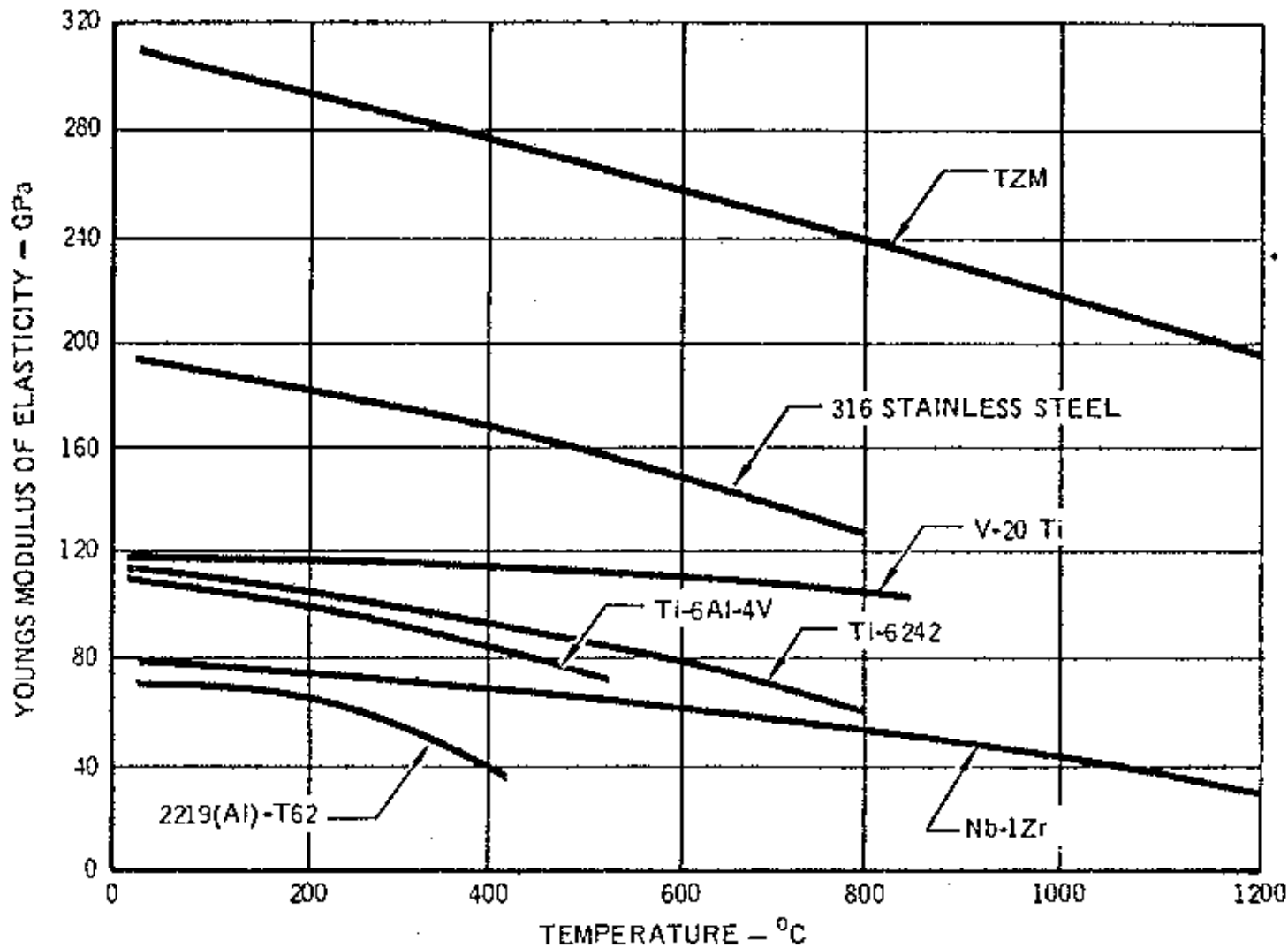
w_s = **surface heat flux**

w_n = **nuclear heat rate**

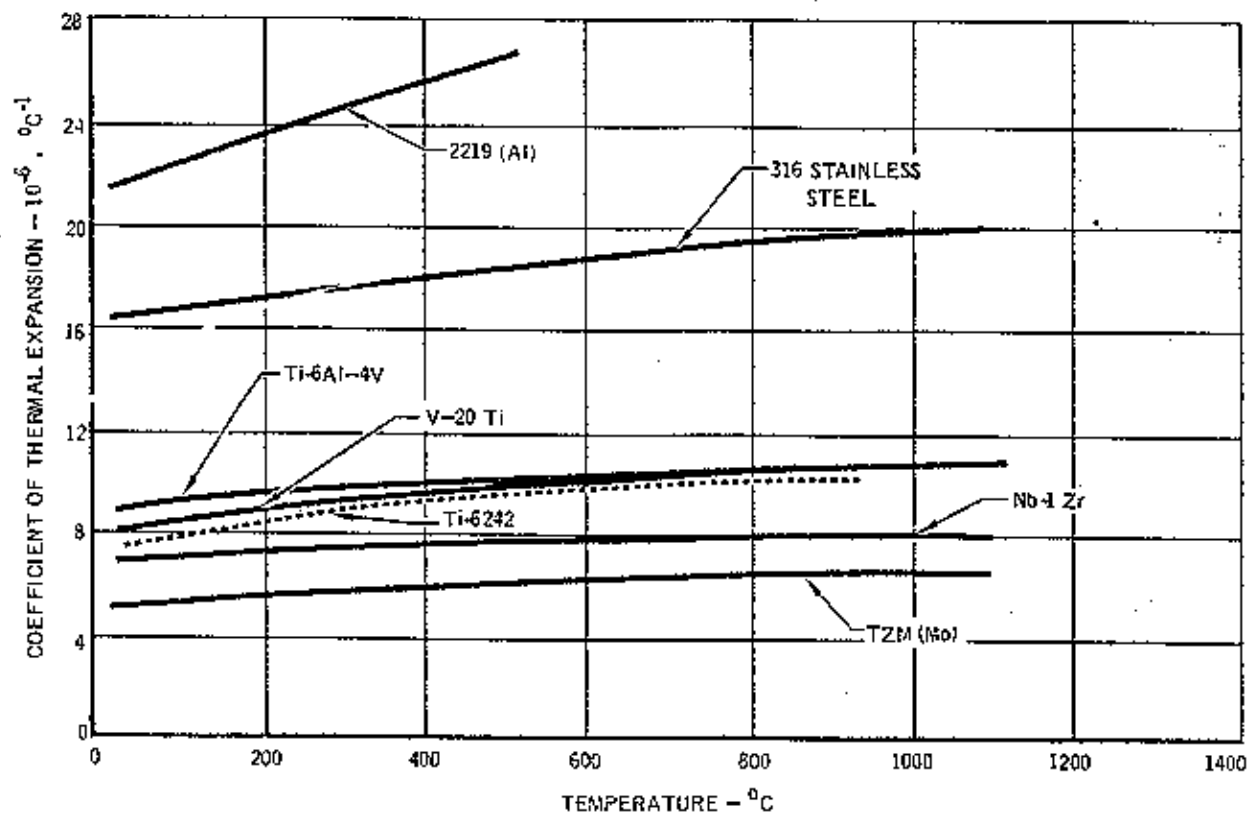
t = **thickness**

$$\text{Figure of Merit} = \frac{\sigma_{th} (T)}{\sigma_y (T)}$$

COMPARISON OF MODULUS OF ELASTICITY FOR SEVERAL CANDIDATE CTR MATERIALS



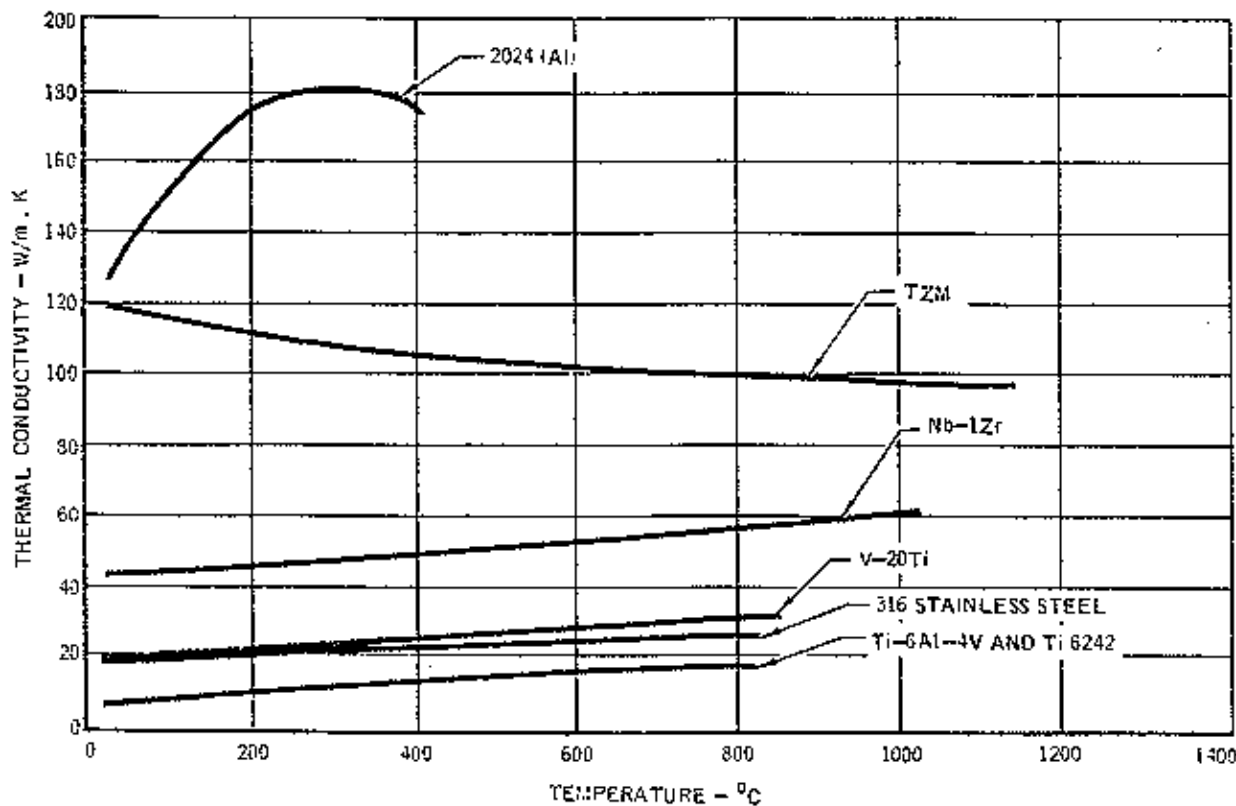
COMPARISON OF THE COEFFICIENT OF THERMAL EXPANSION FOR SEVERAL CANDIDATE CTR MATERIALS



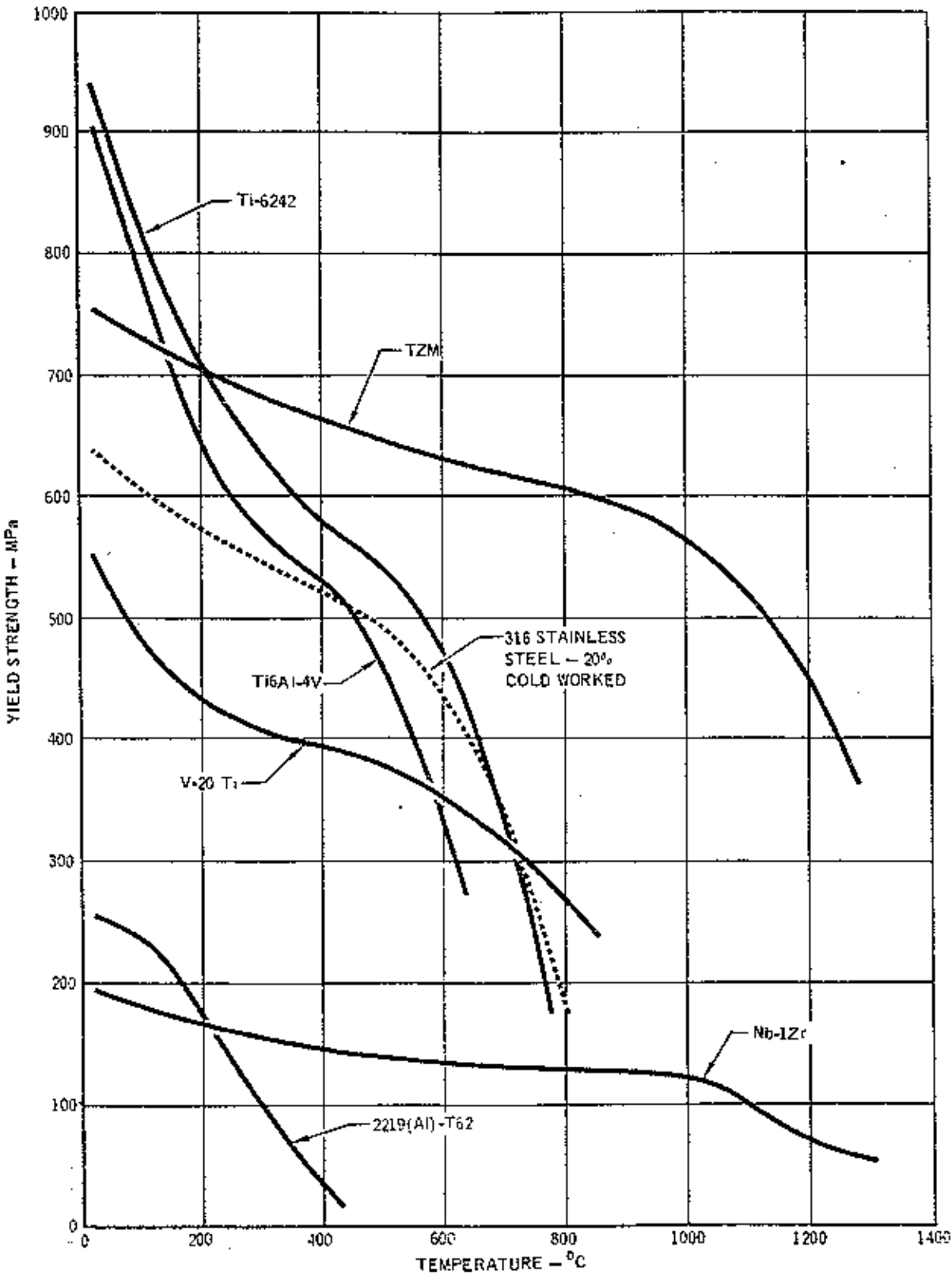
13-187A

Figure 9

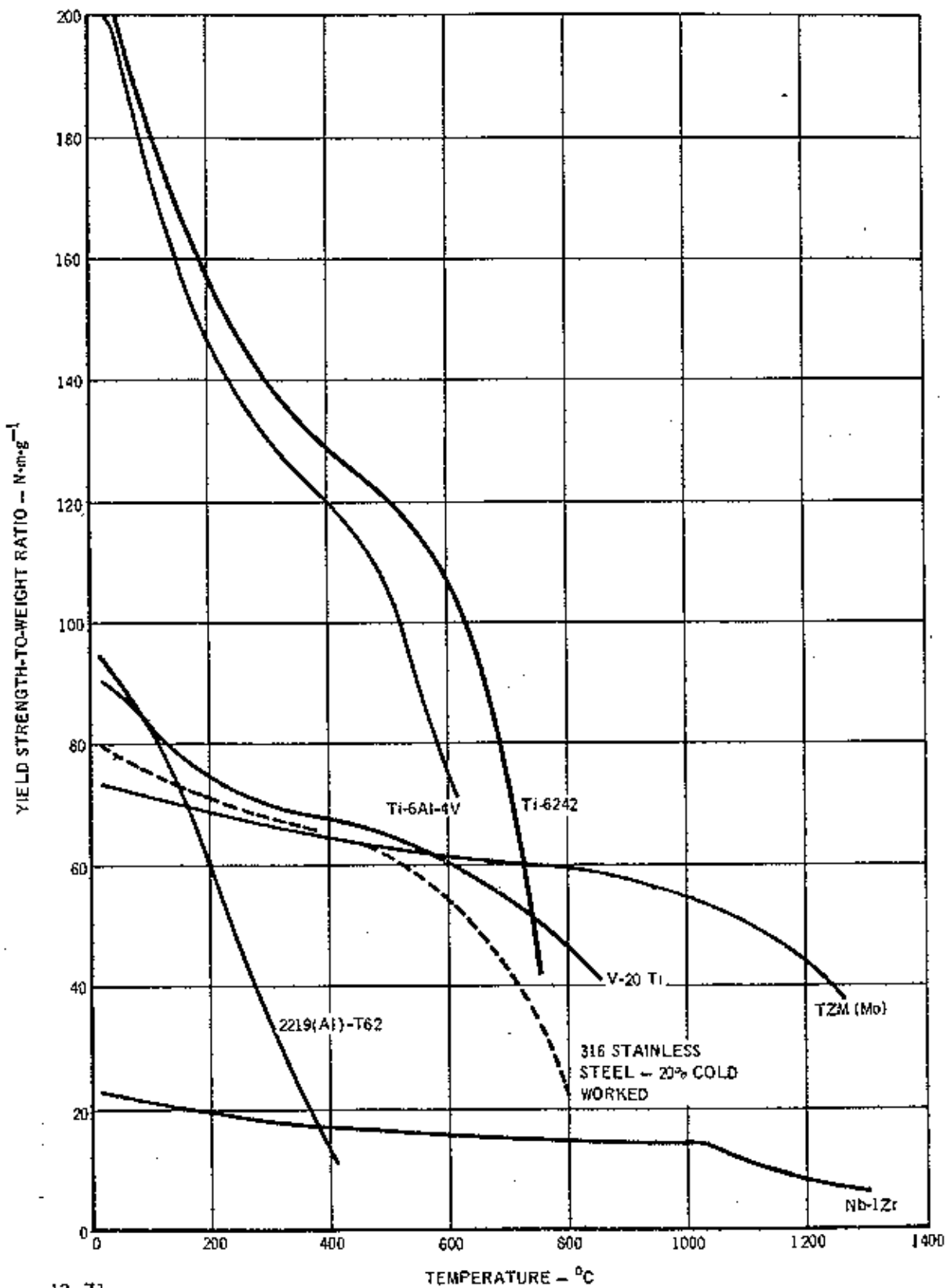
COMPARISON OF THE THERMAL CONDUCTIVITY FOR SEVERAL CANDIDATE CTR MATERIALS



EFFECT OF TEMPERATURE ON THE YIELD STRENGTH OF SEVERAL CANDIDATE CTR MATERIALS



STRENGTH-TO-WEIGHT OF VARIOUS CTR MATERIALS



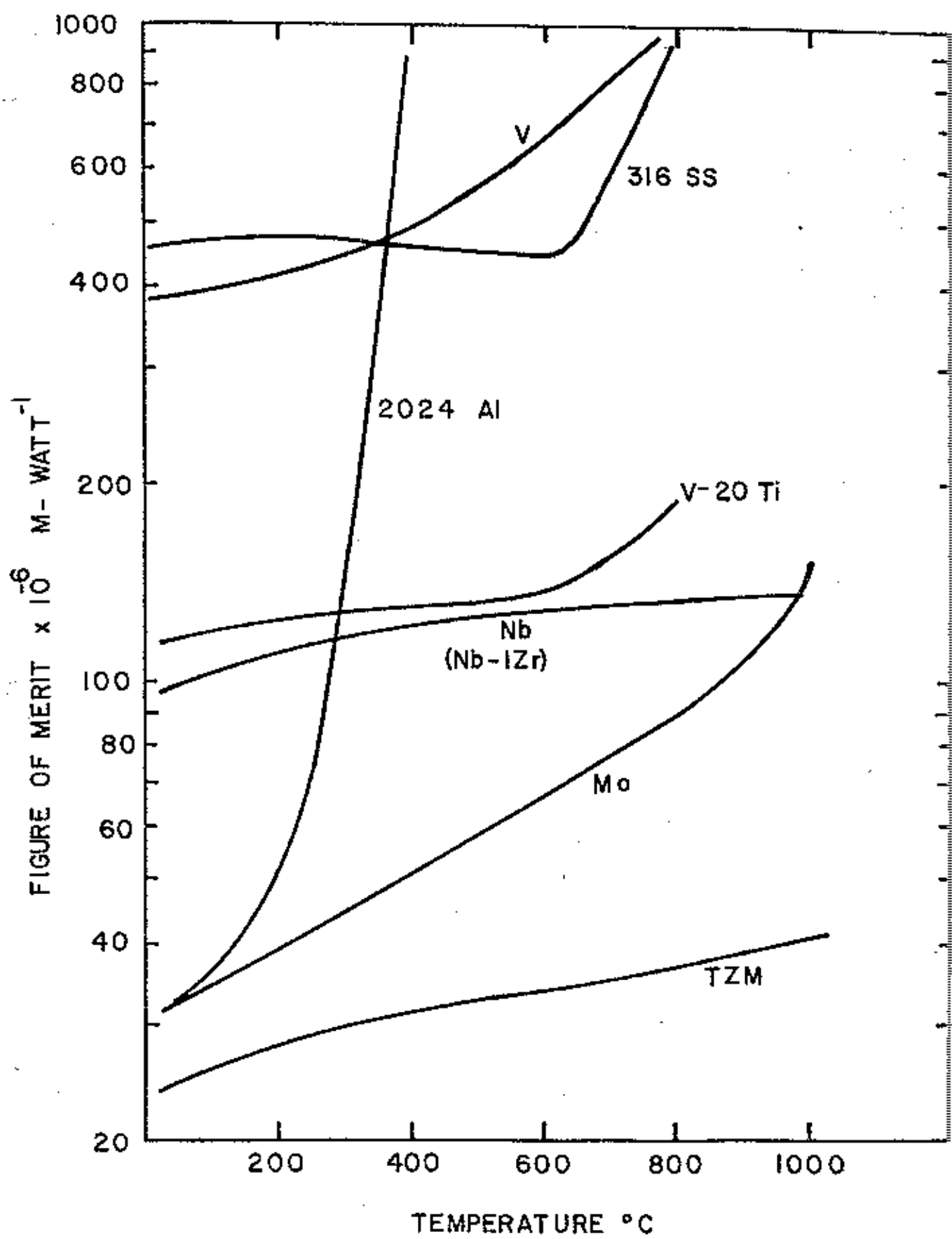
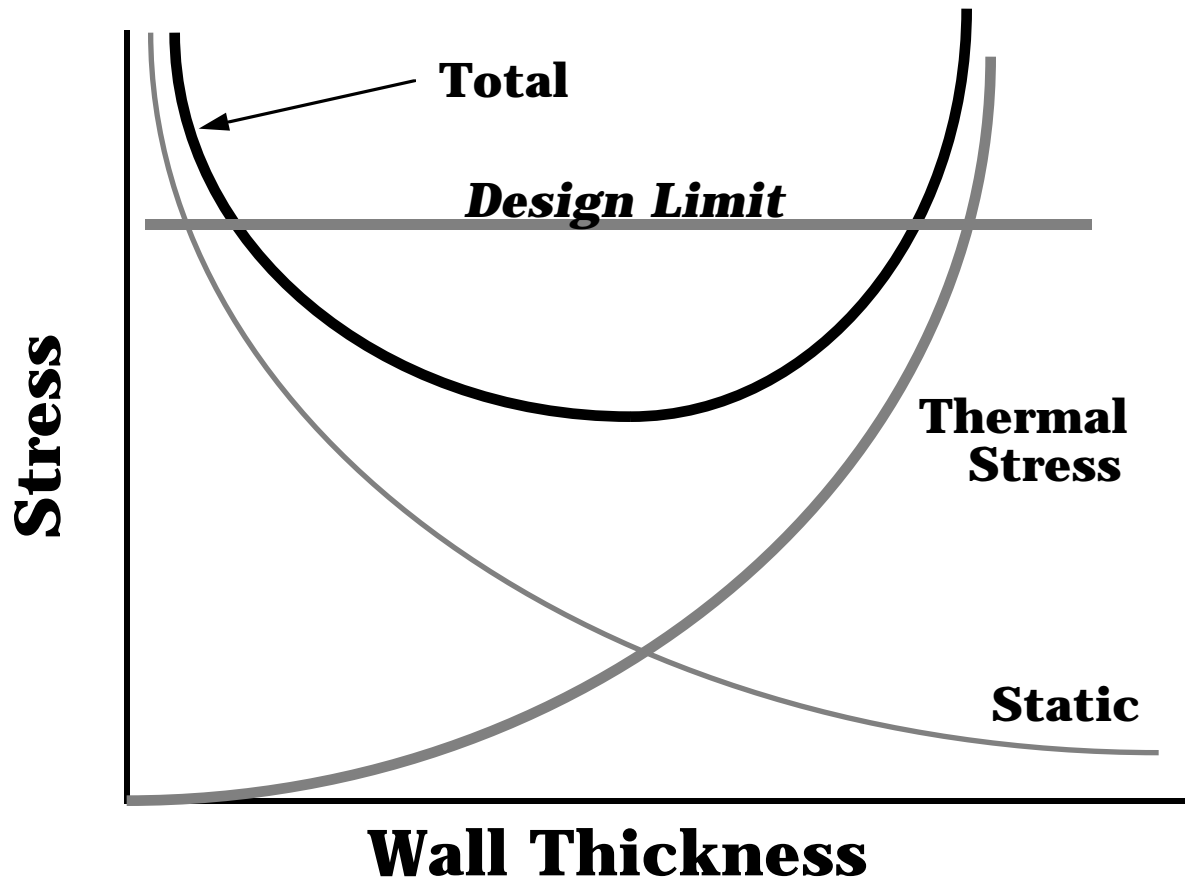


FIG IX-B-12 THERMAL STRESS FIGURE OF MERIT-CTR MATERIAL USING YIELD STRENGTH

First Wall Heat Flux Limits



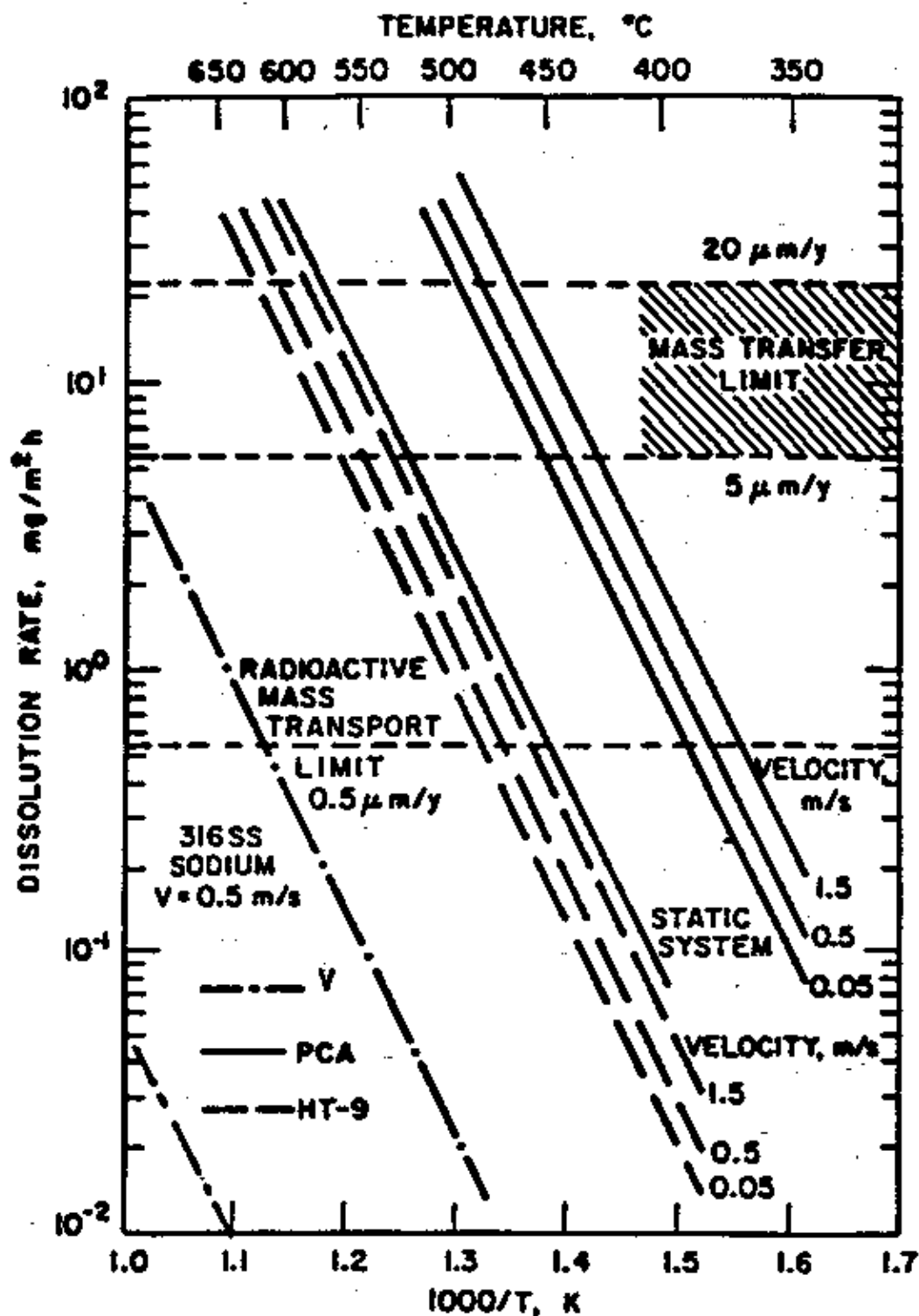


Figure 6.2-4. Effect of temperature on the corrosion rate of PCA and HT-9 alloy in flowing lithium.

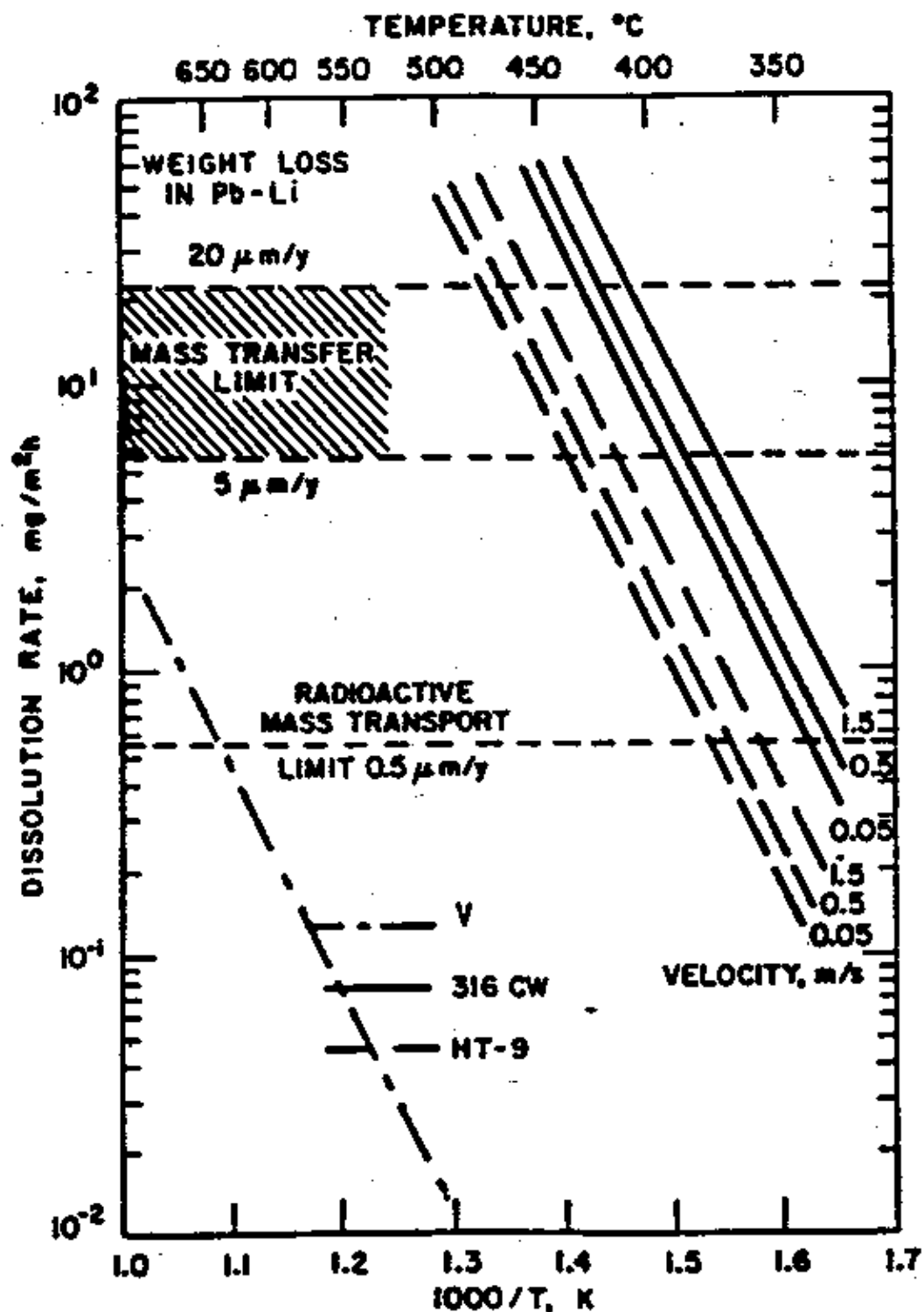


Figure 6.2-5. Effect of temperature on the corrosion rate of 20% cold worked Type 316 stainless steel and HT-9 alloy in flowing Pb-17Li.

TEMPERATURE DEPENDENCE OF THE EQUILIBRIUM DISTRIBUTION COEFFICIENTS FOR OXYGEN BETWEEN SELECTED REFRACTORY METALS AND LITHIUM

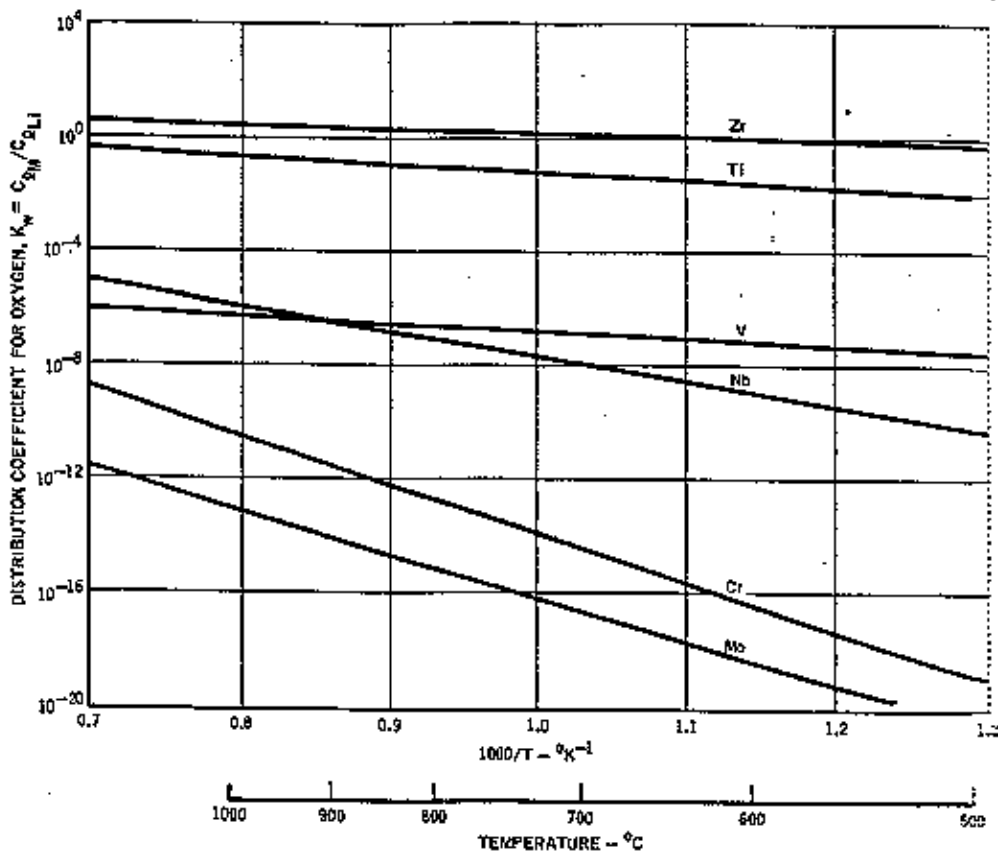
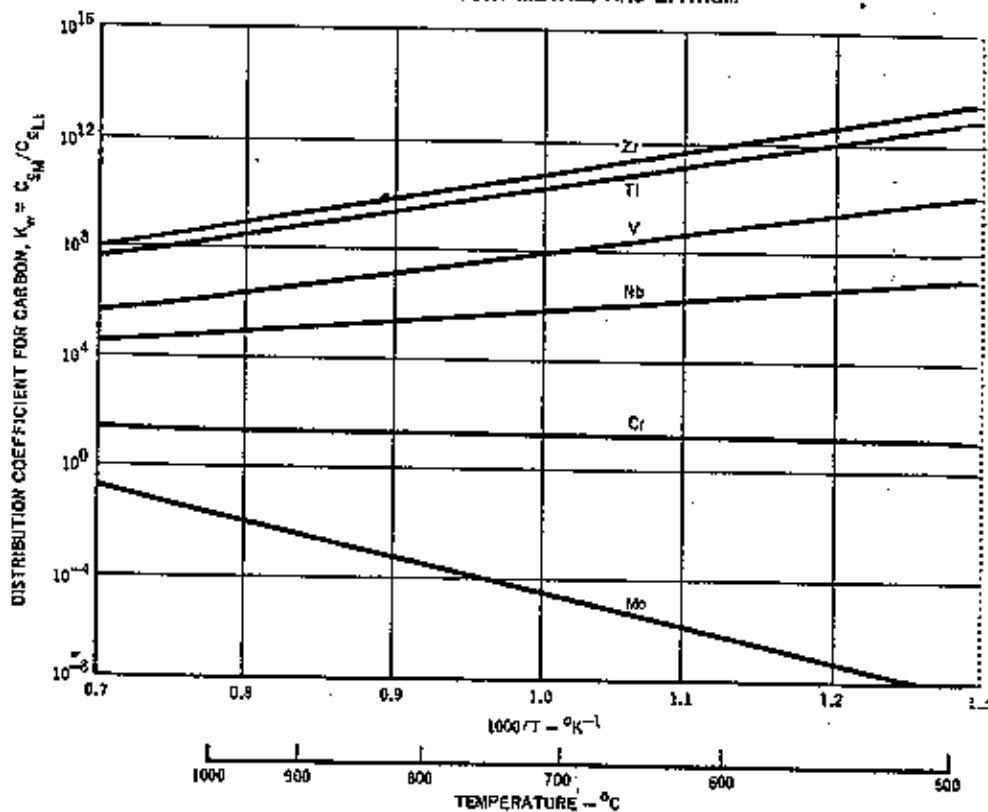


Figure 28

TEMPERATURE DEPENDENCE OF THE EQUILIBRIUM DISTRIBUTION COEFFICIENTS FOR CARBON BETWEEN SELECTED REFRACTORY METALS AND LITHIUM



Compatibility Limits

<u>Alloy</u>	<u>Coolant</u>	<u>Tmax °C</u>
Al	Li	< 200
316 SS	Li	< 550
HT-9	Li	< 550
V	Li	< 800
Nb	Li	< 800
Mo	Li	< 1000

316 SS	Pb-Li	< 450
HT-9	Pb-Li	< 500
V	Pb-Li	????
Nb	Pb-Li	????
Mo	Pb-Li	????

316 SS/HT-9	Helium	< 600
V, Nb	Helium	< 600
Mo	Helium	< 1000

Radiation Damage in Fusion Reactor Materials

Atomic
Reactions

Nuclear
Reactions

Displacements

Transmutations

Sputtering

Resistivity
Increases

Radioactivity

Afterheat

Chemical
Change

- Swelling

- Ductility Loss

- Increased Crack Propagation

- Increased Creep Rates

Fundamentals of Radiation Damage

Number of Vacancy/Interstitial Pairs produced by the *i*th reaction per incident particle of energy *E* per second, $N_d^i(E)$

$$N_d^i(E) = N_o \int \phi(E) \sigma^i(E) K(E, T) \nu(T) dT$$

Where:

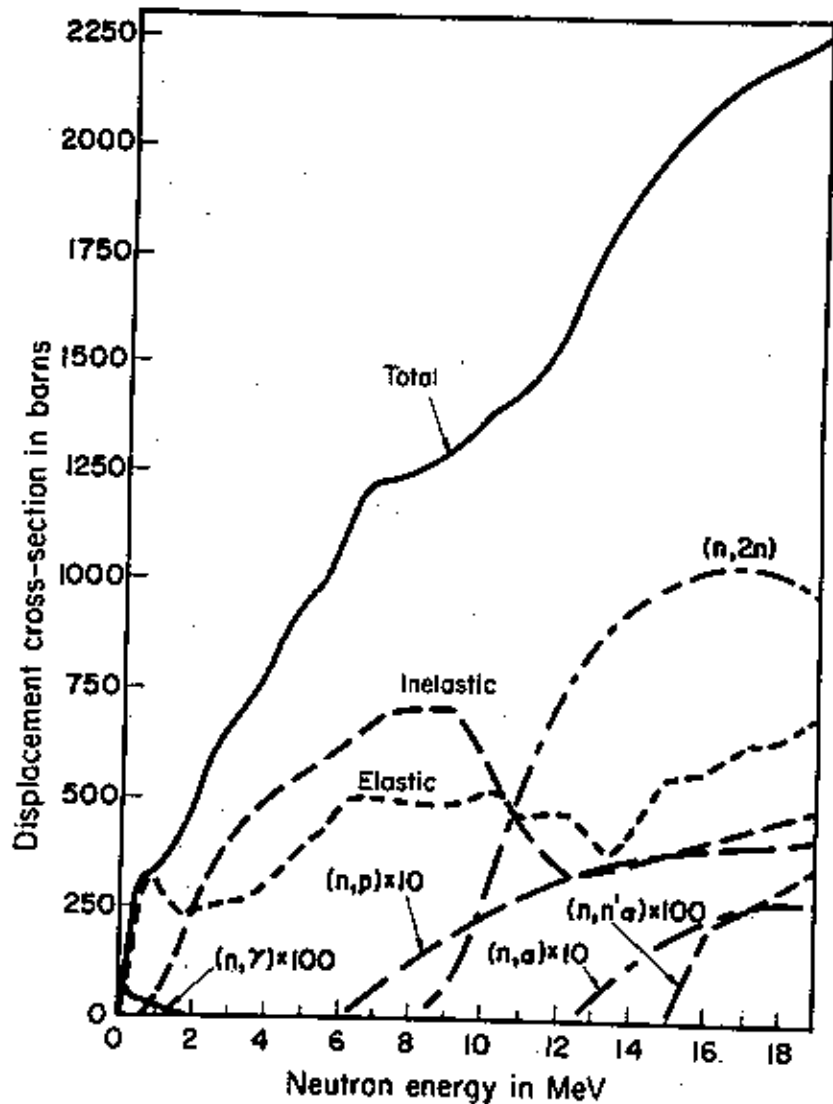
N_o = Atomic Density

$\phi(E)$ = Flux of particles of energy *E*

$\sigma^i(E)$ = Probability that the incident particle with energy *E*, causing reaction *i*, will undergo an interaction with a matrix atom

$K(E, T)$ = Probability that if an interaction takes place, it will produce a primary knock-on-atom (PKA) with energy *T*

$\nu(T)$ = Number of atoms subsequently displaced by the PKA



Individual contributions to the total niobium displacement cross-section.

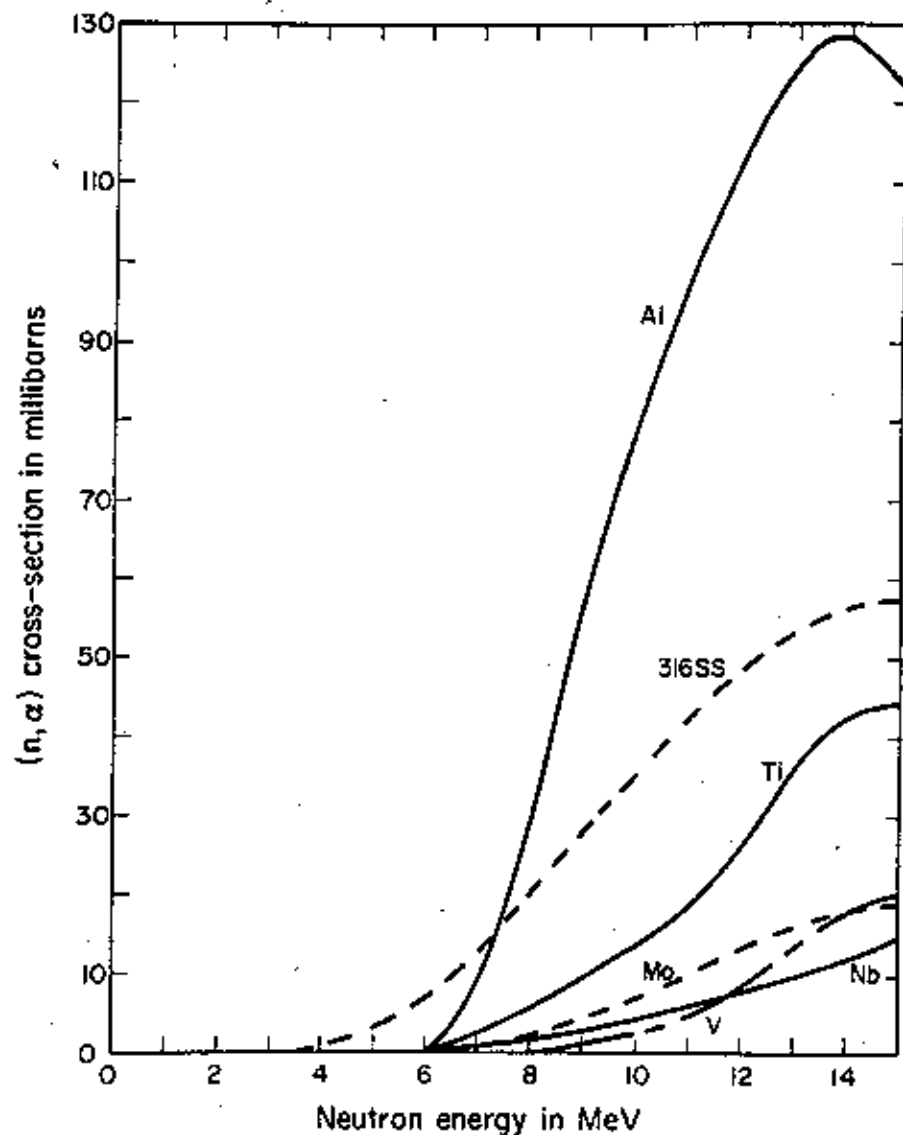
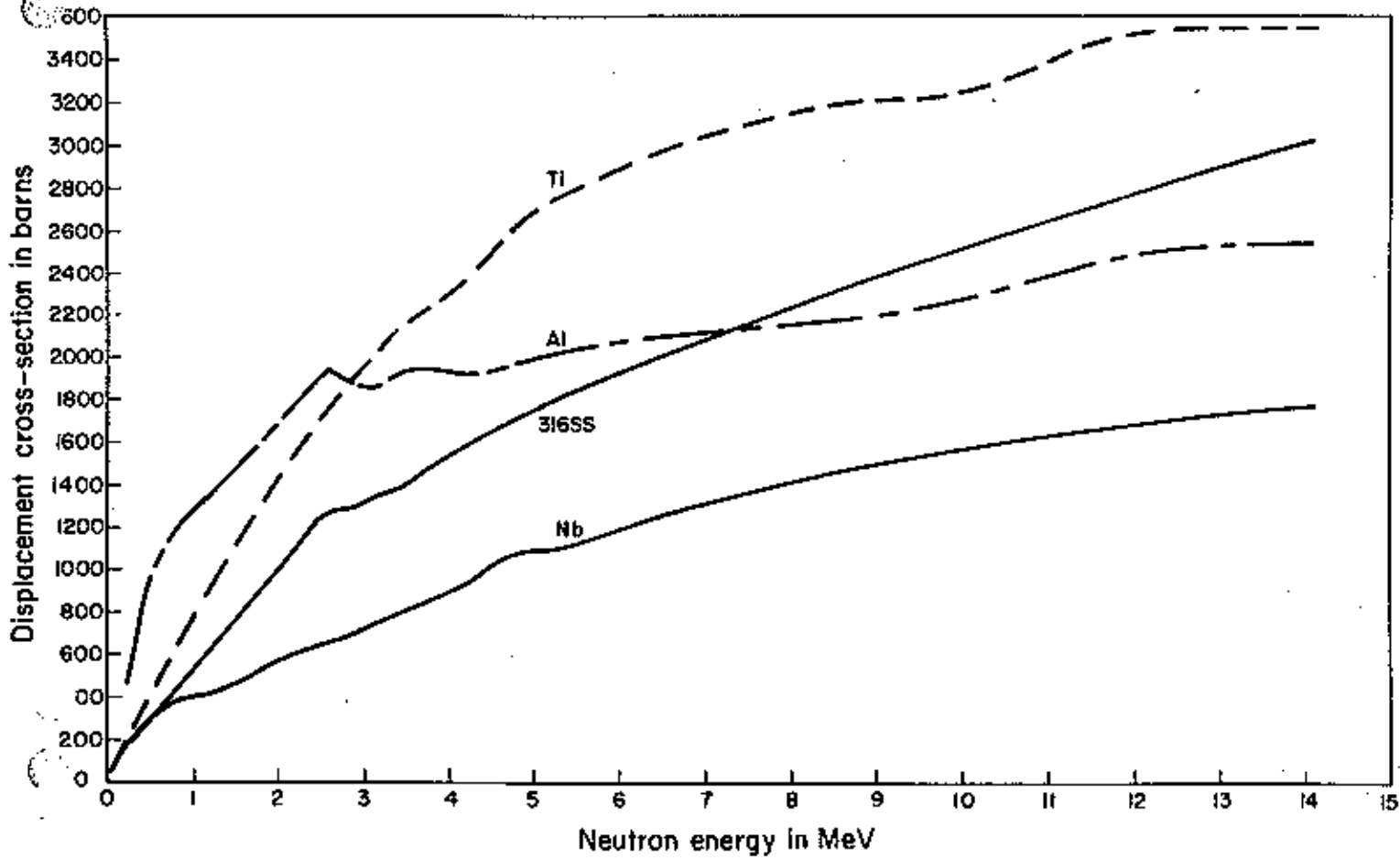
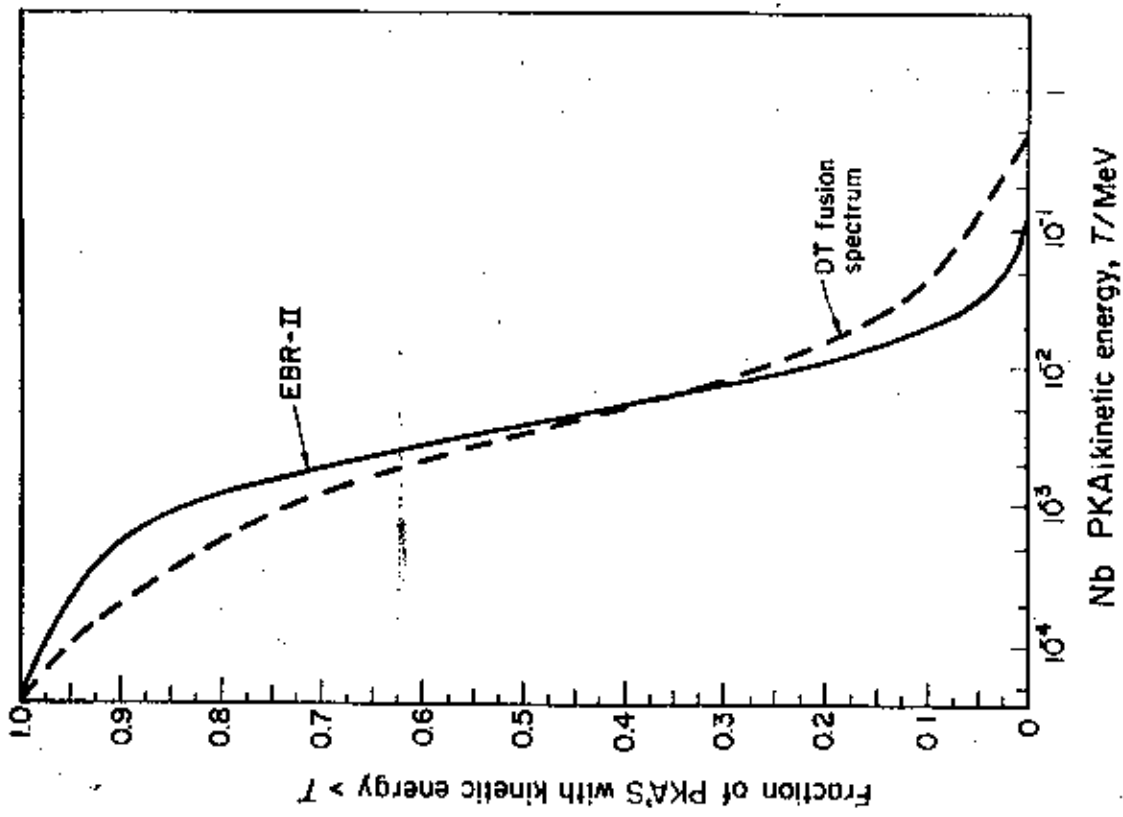


Figure 15. Helium gas production cross-section.



Displacements per $\frac{MW}{m^2}$

Definition of dpa (displacements per atom) is the number of times that an atom is displaced for a given fluence.

$$\frac{N_d}{N_o} = \phi t \sigma_d$$

Example of 1 $\frac{MW}{m^2}$

$$\phi = 4.43 \times 10^{13} \frac{n}{cm^2 - s}$$

$$\sigma_d = 3,000b$$

$$\frac{N_d}{N_o t} = 4.43 \times 10^{13} \cdot 3 \times 10^{-21}$$

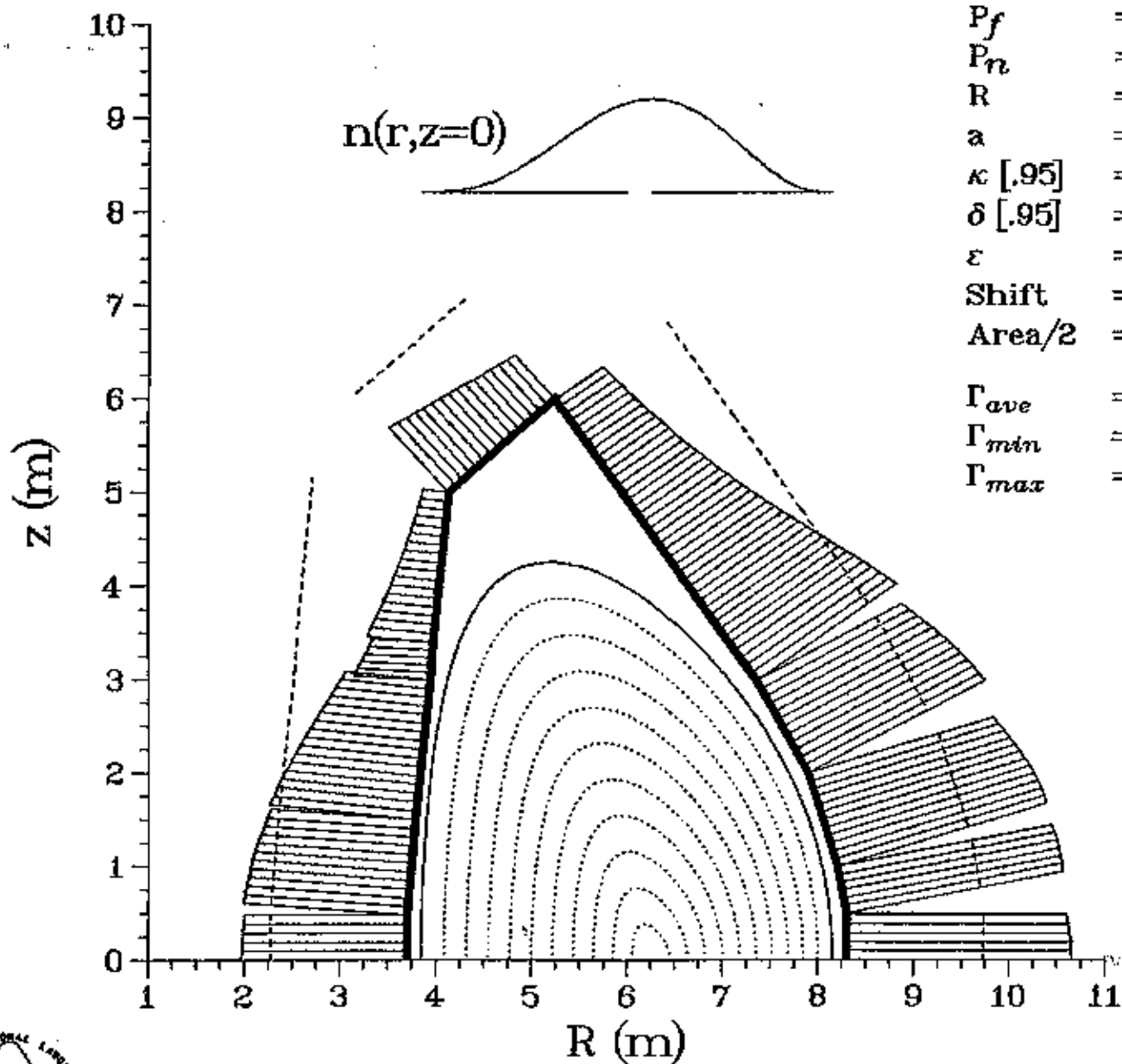
$$= 1.3 \times 10^{-7} \frac{dpa}{s}$$

$$\approx 4 \frac{dpa}{FPY}$$

Damage Rate in CTR materials	
Material	dpa/FPY per MW/m ²
316 SS	10
V	12
Mo	8
SiC	30
Al	17

ITER Neutron Wall Loading Distribution

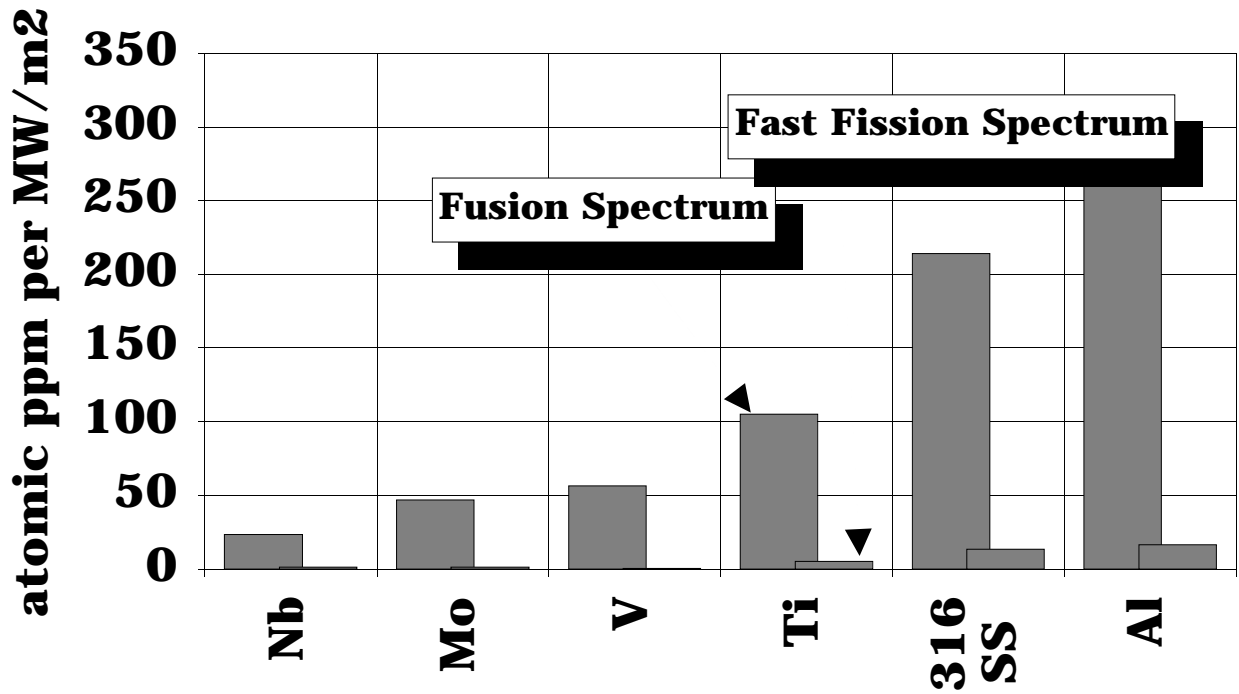
Physics Phase 1100 MW



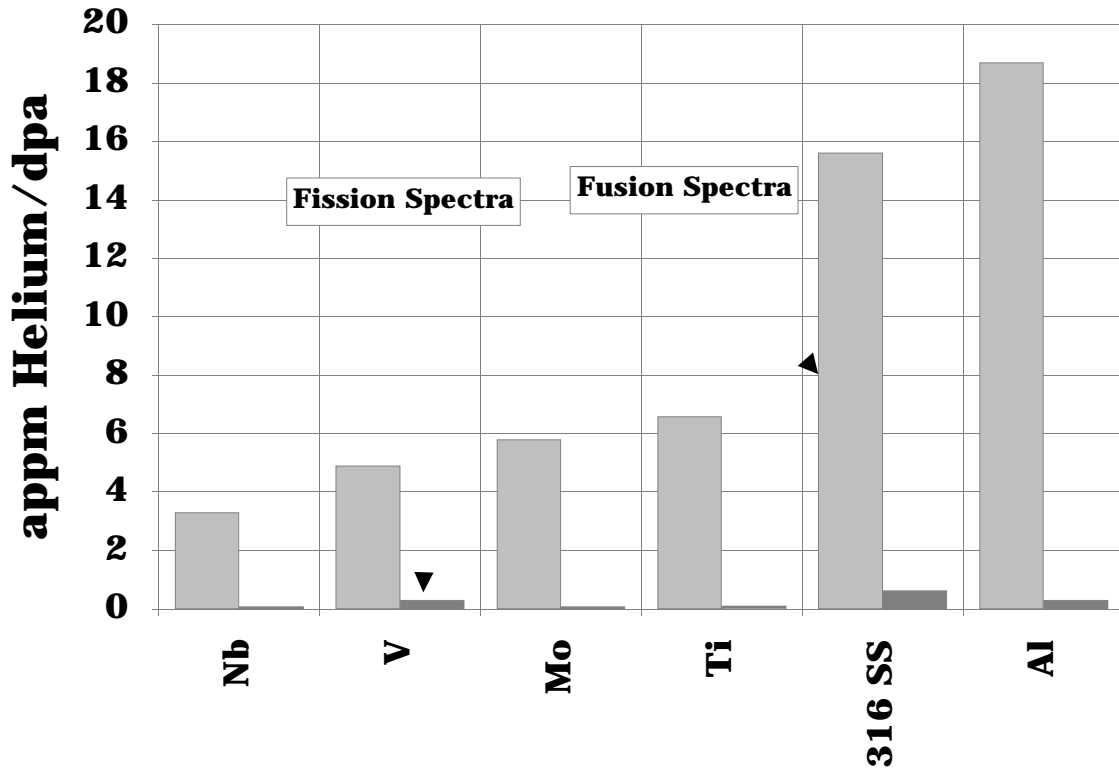
P_f	=	1100.
P_n	=	881.25
R	=	6.
a	=	2.15
κ [.95]	=	1.982
δ [.95]	=	0.383
ε	=	3.
Shift	=	0.255
Area/2	=	471.836
Γ_{ave}	=	0.934
Γ_{min}	=	0.175
Γ_{max}	=	1.54



The Production of Helium Gas in Metals and Alloys is much Greater than in Fission Reactors



The Helium to Dpa Ratio is Much Higher in Fusion Reactors Than in Fission Systems



Swelling

- **First discovered in 1986-UK**
- **Occurs when vacancies collect into clusters which grow and cause the material to expand**
- **Has been observed in many pure metals and alloys (Mg, Al, V, Fe, Co, Ni, Cu, Nb, Mo, Ta, W, Re, and Pt) and dozens of alloys.**
- **Generally occurs between 30 and 50% of the absolute melting point.**

(Figures)

- **Usually try to keep swelling <<10% (i.e., 1-2%)**
 - **Limits the operating life to 2-3 FPY's in austenitic steels and 5-7 FPY's in ferritic steels.**
-

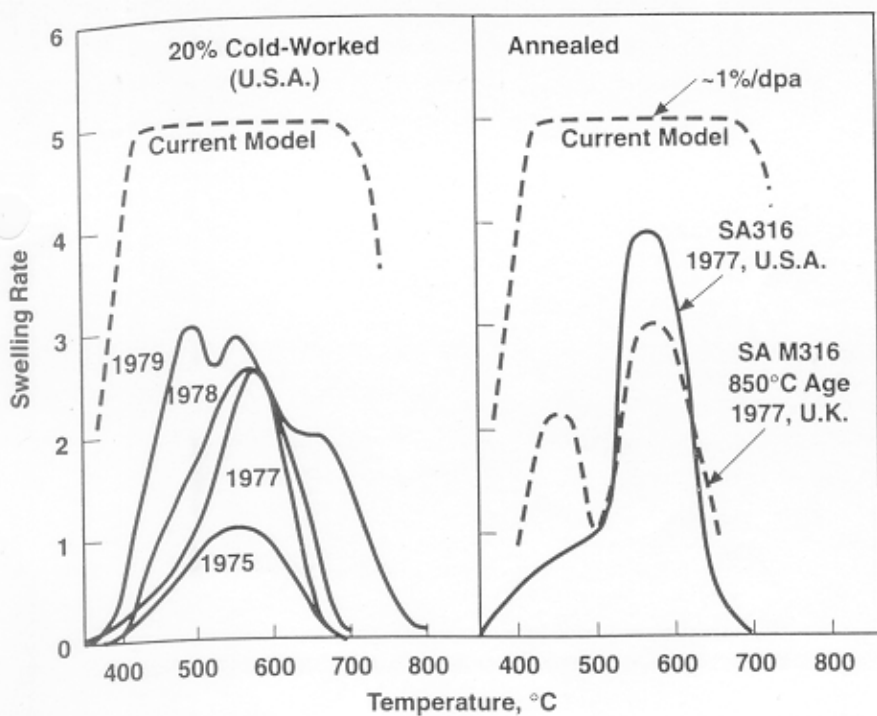


Figure 6-22. Chronological evolution of swelling predictions for AISI 316 in the U.S. LMR materials program, reflecting the tendency of predictions to increase as data became available at progressively higher swelling levels (Garner, previously unpublished). The swelling rate is in units of $\%/10^{22} \text{ n cm}^{-2}$ ($E > 0.1 \text{ MeV}$).

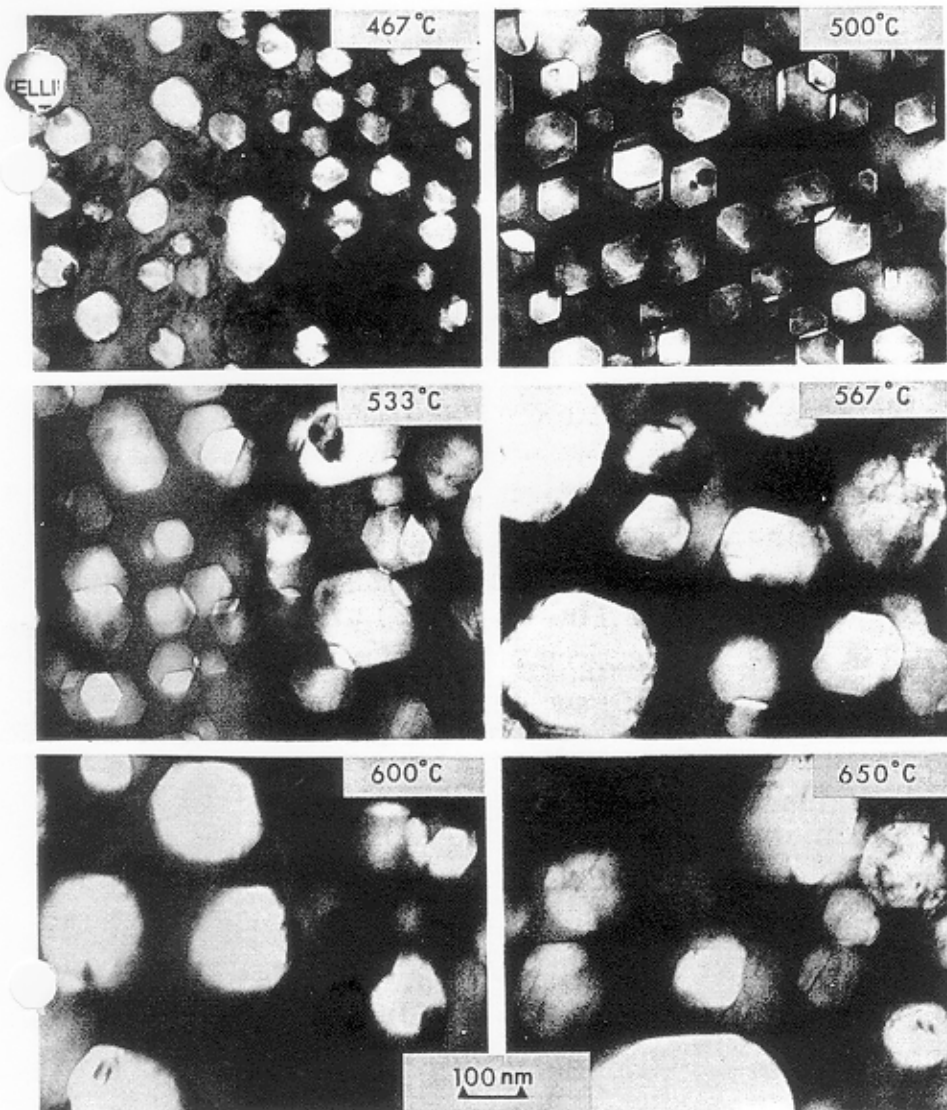


Figure 6-23. Temperature dependence of void swelling observed in FFTF first core heat CN-13 of 20% cold worked AISI 316 at $\approx 1.4 \times 10^{23} \text{ n cm}^{-2}$ ($E > 0.1 \text{ MeV}$) or $\approx 70 \text{ dpa}$ (courtesy of W. J. S. Yang of Westinghouse Hanford Company).

20% CW 316

1 cm

UNIRRADIATED
CONTROL

FLUENCES
BEYOND
FFTF
GOAL

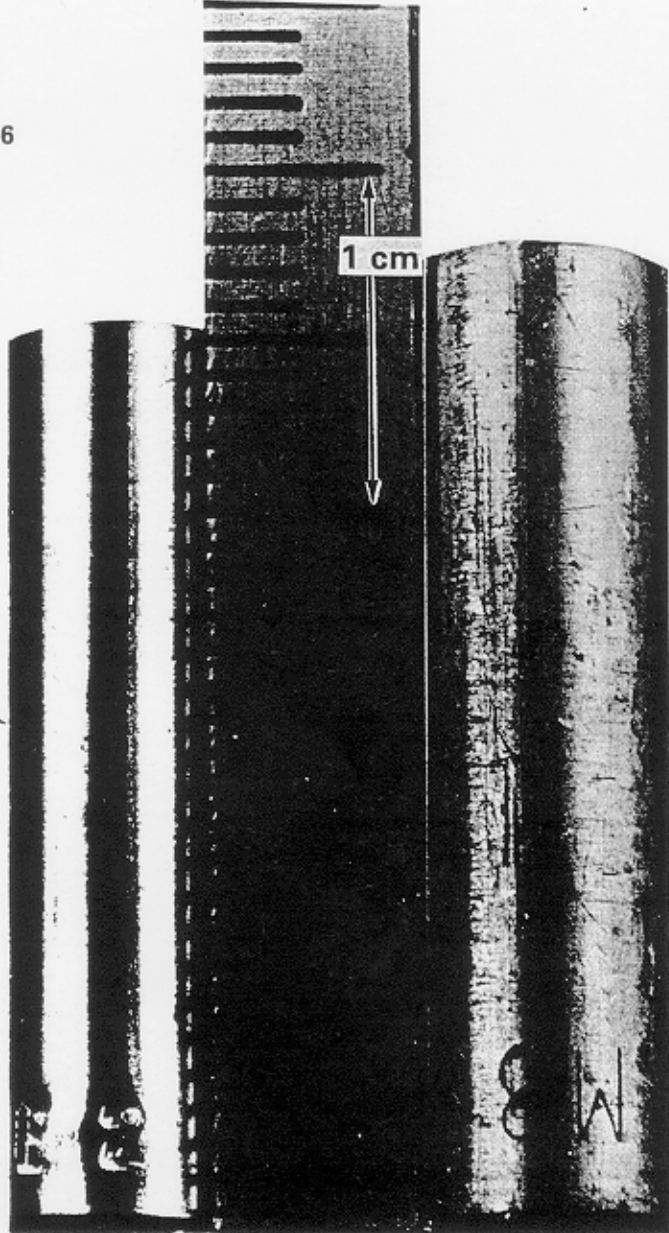


Figure 6-24. Easily observed swelling ($\approx 10\%$ linear, $\approx 33\%$ volumetric) in unfueled 20% cold worked AISI 316 cladding tube at $1.5 \times 10^{23} \text{ n cm}^{-2}$ ($E > 0.1 \text{ MeV}$) or $\approx 75 \text{ dpa}$ at 510°C in EBR-II (after Straalsund et al., 1982). Note that, in the absence of physical restraints, all relative proportions are preserved during swelling.

SWELLING ESTIMATES OF TYPE 316
STAINLESS STEEL, 20% COLD WORKED
(AUG. 1969)

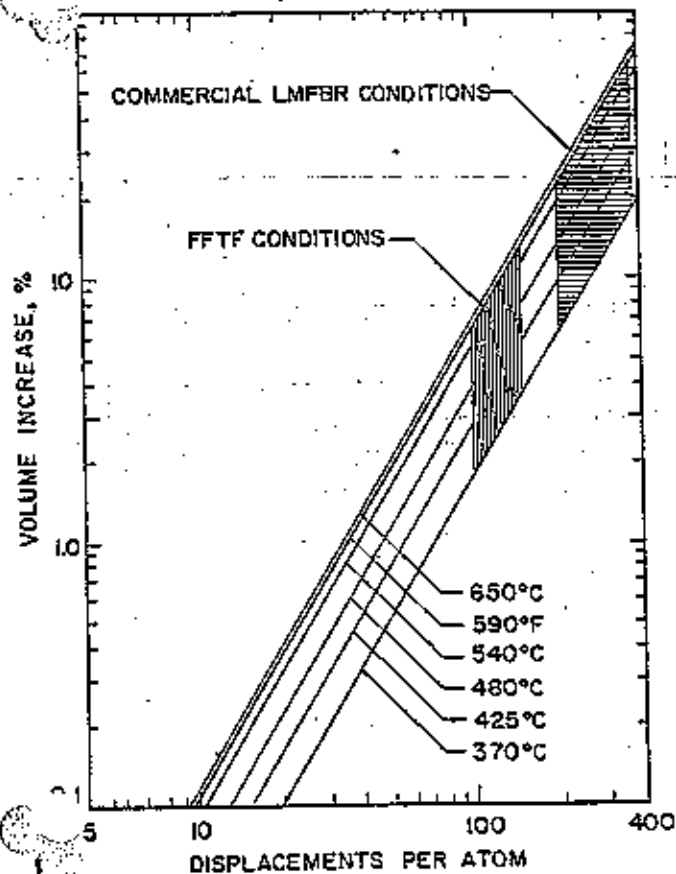
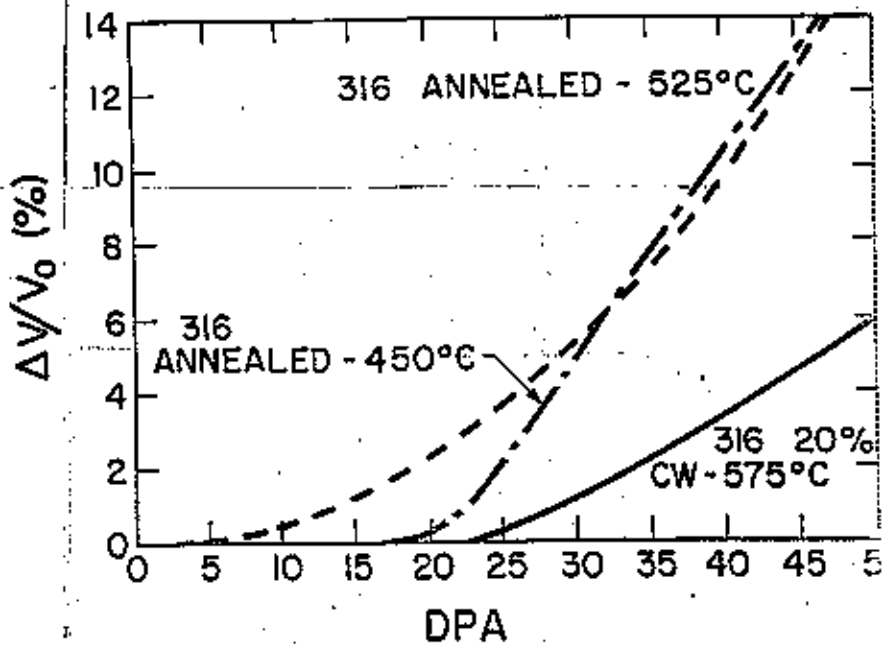
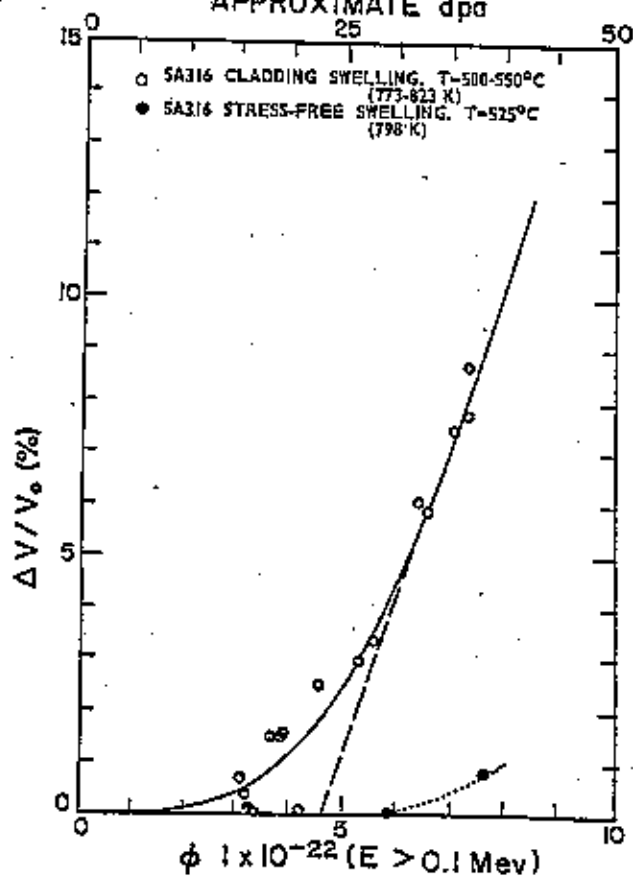


FIGURE 5

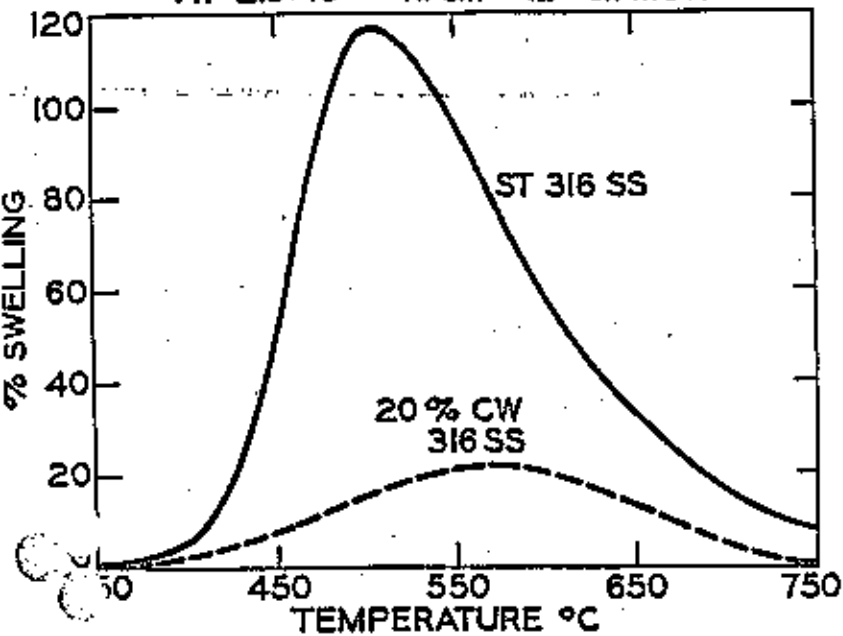


TYPICAL SWELLING IN AUSTENITIC STEELS

FIGURE 21 STRESS EFFECT ON SWELLING - WEINER & BOLTAX
APPROXIMATE dpa



PREDICTED SWELLING FOR
SOLUTION TREATED 316 STAINLESS STEEL
AT 2.5×10^{23} n/cm² (E > 0.1 MeV)



Embrittlement

- **Loss of ductility due to helium collecting at grain boundaries.**
- **Try to keep the uniform elongation > 1%**
- **In ferritic steels, the shift in the ductile to brittle transition temperature is the important thing.**

(Figures)

Overall Conclusions

- **In DT devices , displacement and transmutation effects will limit useful lifetimes to a few full power years. Hence replacement of the FW, blanket, components will have to be done on a regularly scheduled basis.**
- **Use of advanced fuels will drop the neutron wall loading by a factor of ≈ 30 which means that the structural materials can last for the life of the reactor.**

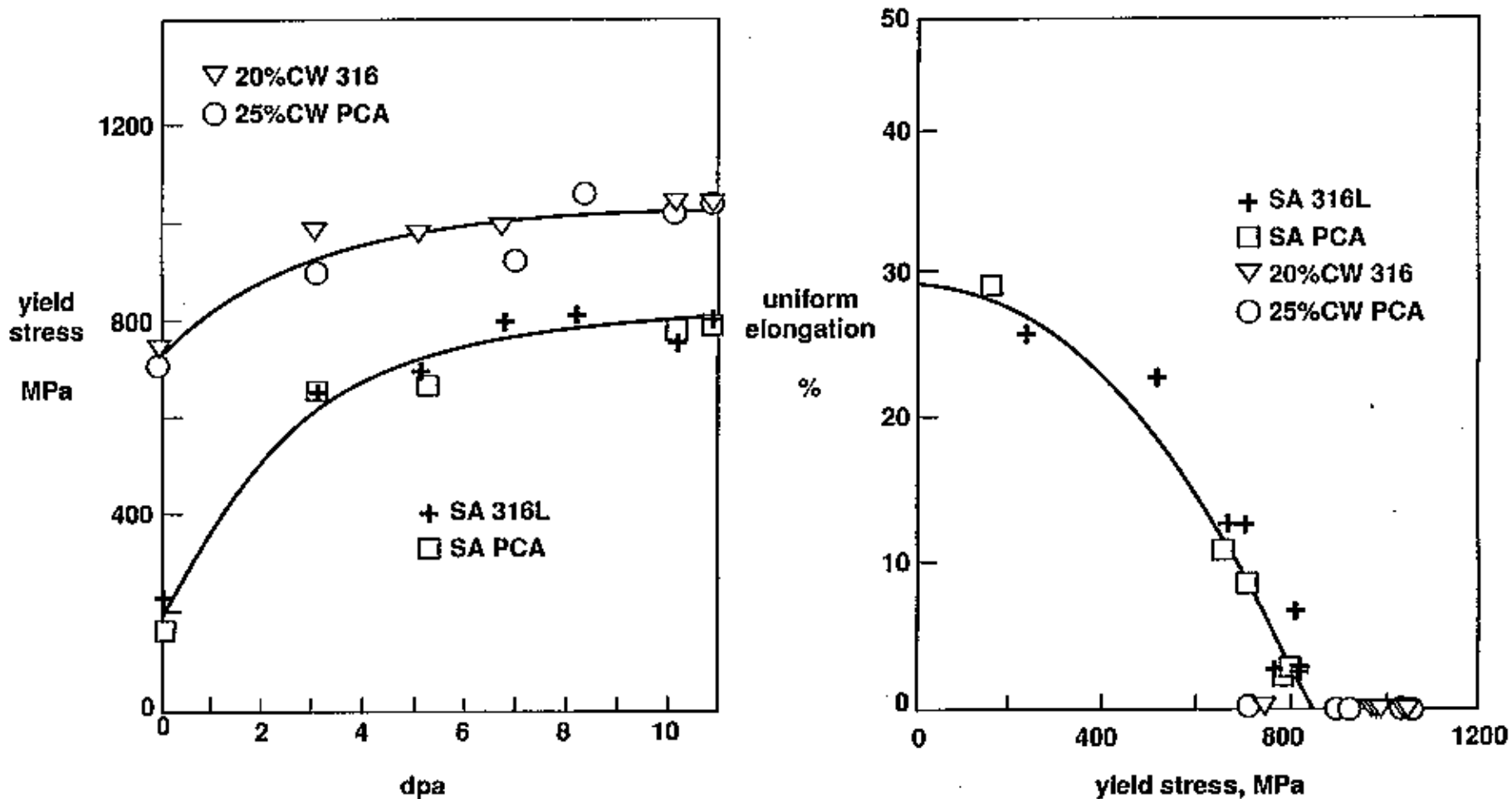


Figure 6-146. Hardening and ductility loss observed in two stainless steels irradiated in the HFIR, HFR, and R2 mixed spectrum reactors at 250°C at helium/dpa ratios ranging from 10 to 35 appm/dpa (after Elen and Fenici, 1992).

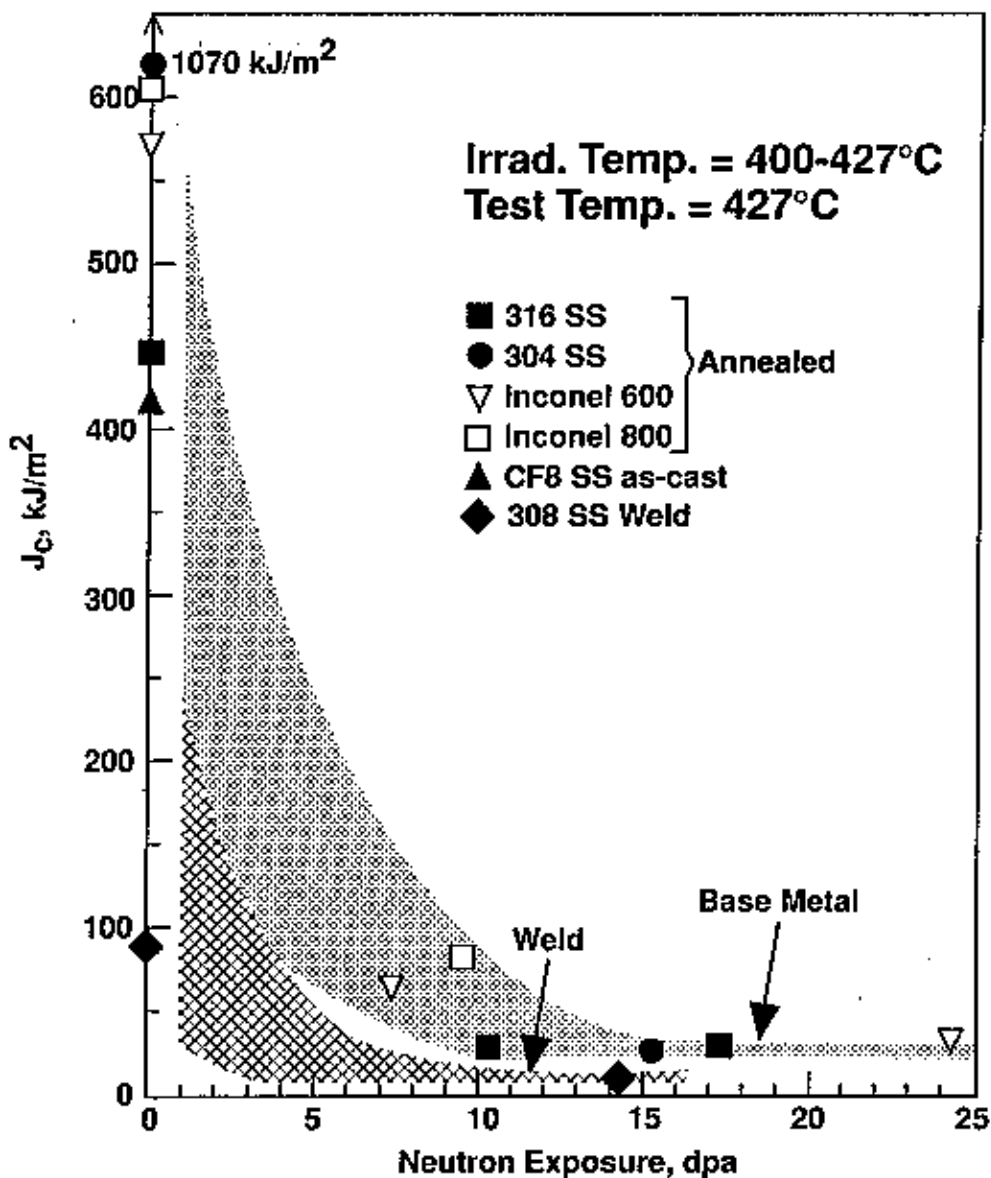


Figure 6-163. Irradiation-induced evolution of J_c fracture toughness in various austenitic steels and welds (after Mills, 1982).

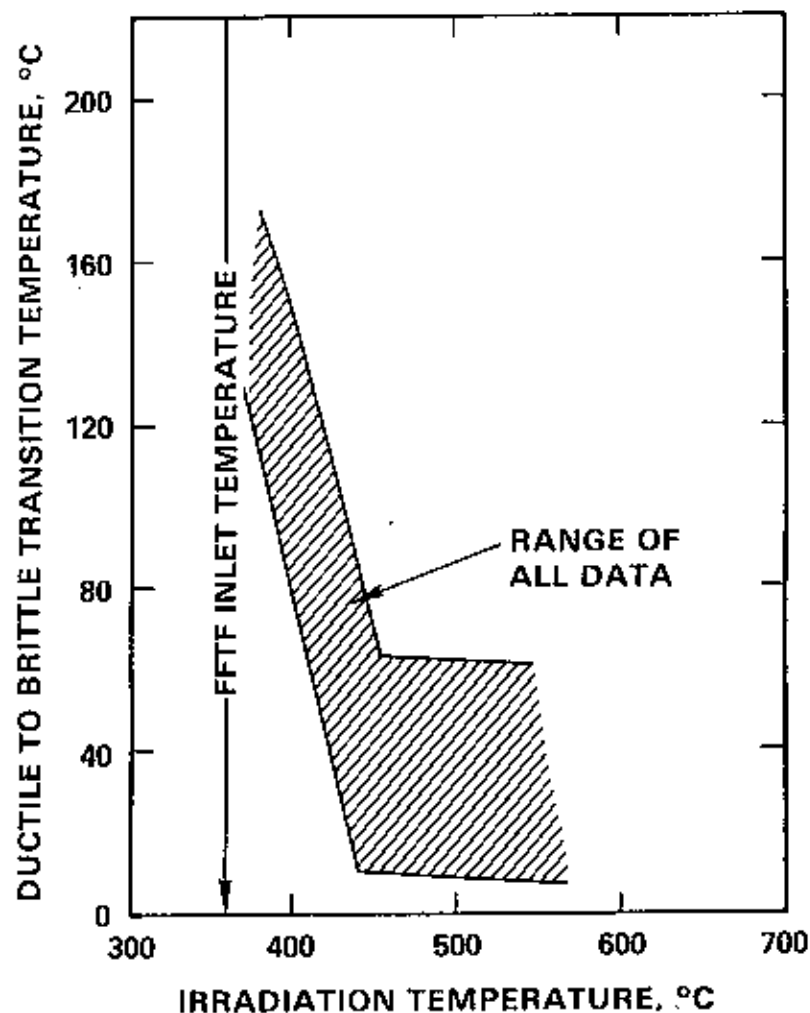


Figure 6-168. Dependence of DBTT on irradiation temperature for HT9 irradiated in FFTF (unpublished data courtesy of W. L. Hu, Westinghouse Hanford Company).

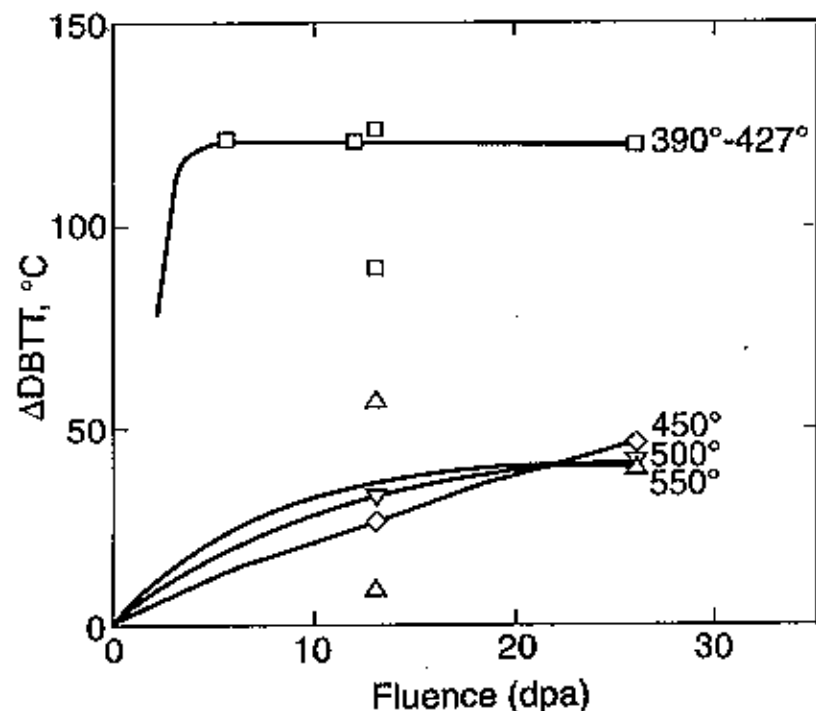


Figure 6-170. Shift in ductile to brittle transition temperature in HT9 as a function of neutron fluence and irradiation temperature (after Powell et al., 1986).

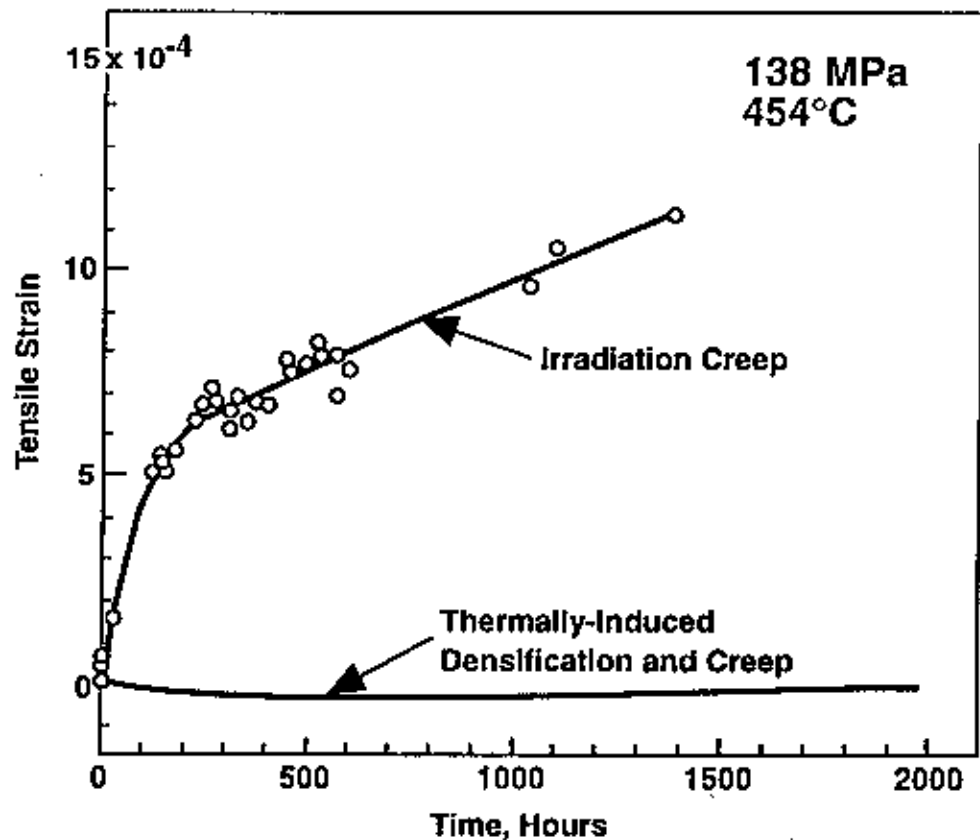


Figure 6-92. Comparison of creep rates observed in 20% cold worked 316 stainless steel in uniaxial tests during thermal aging or neutron irradiation in EBR-II (after Gilbert et al., 1972).

Criteria for Selecting First Wall Materials in Fusion Reactors*

Criteria	Favored Materials	Less Favored
<p style="text-align: center;">Radiation Damage and Lifetime</p> <p>1) Swelling 2) Embrittlement</p>	Ti, FS**, V, Mo, AS** AS, Ti	Al, C, SiC FS, V, Mo, C, SiC
<p style="text-align: center;">Chemical Compatibility</p> <p>1) Lithium 2) Helium (impurities) 3) Pb-Li Alloys 4) Water</p>	Mo, V, FS, AS, Ti Mo, FS, AS, C, SiC Mo, V, FS, AS, Ti, SiC, C AS, FS, Mo, Ti, Al	(SiC, Al, C) Ti, Al, (V) Al V, (SiC, C)
<p style="text-align: center;">Mechanical and Thermal</p> <p>1) Yield Strength 2) Embrittlement 3) Creep Strength 4) Thermal Stress</p> $= \frac{2\sigma_y k(1-\nu)}{\alpha E}$	Mo, Ti, V, FS, AS AS, Ti, Al, Mo, FS Mo, V, FS, AS, Ti Mo, Al, V	SiC, C, Al V, SiC, C C, SiC, Al Ti, FS, AS
<p style="text-align: center;">Fabricability and Joining</p>	AS, Al, FS, Ti	V, Mo, C, SiC
<p style="text-align: center;">Database and Industrial Capability</p>	AS, FS, Al, Ti, C	SiC, Mo, V
<p style="text-align: center;">Long-lived Radioactivity</p>	V, C, SiC, Ti, Al	FS, AS, Mo
<p style="text-align: center;">Cost</p>	Al, AS, FS, C	Ti, V, SiC, Mo
<p style="text-align: center;">Resource Availability (USA)</p>	C, SiC, Al, Ti, Mo, AS, FS	V

* Note: Only Base Metal Listed (i.e., Ti for Ti alloys, V for V alloys, etc.)

** AS for austenitic stainless steel, FS for ferritic steel

() Materials in parentheses are generally unacceptable with coolant.